

# Development of gallium oxide power devices

## Invited Article

Masataka Higashiwaki<sup>\*1</sup>, Kohei Sasaki<sup>1,2</sup>, Akito Kuramata<sup>2</sup>, Takekazu Masui<sup>3</sup>, and Shigenobu Yamakoshi<sup>2</sup>

<sup>1</sup> National Institute of Information and Communications Technology, 4-2-1 Nukui-Kitamachi, Koganei, Tokyo 184-8795, Japan

<sup>2</sup> Tamura Corporation, 2-3-1 Hirose-dai, Sayama, Saitama 350-1328, Japan

<sup>3</sup> Koha Co., Ltd., 2-6-8 Kouyama, Nerima, Tokyo 176-0022, Japan

Received 3 August 2013, revised 22 October 2013, accepted 22 October 2013

Published online 21 November 2013

**Keywords** field-effect transistors, Ga<sub>2</sub>O<sub>3</sub>, MESFET, molecular beam epitaxy, power devices, Schottky barrier diodes

\* Corresponding author: mhigashi@nict.go.jp, Phone: +81-42-327-6092, Fax: +81-42-327-6669

Gallium oxide (Ga<sub>2</sub>O<sub>3</sub>) is a strong contender for power electronic devices. The material possesses excellent properties such as a large bandgap of 4.7–4.9 eV for a high breakdown field of 8 MV cm<sup>-1</sup>. Low cost, high volume production of large single-crystal β-Ga<sub>2</sub>O<sub>3</sub> substrates can be realized by melt-growth methods commonly adopted in the industry. High-quality n-type Ga<sub>2</sub>O<sub>3</sub> epitaxial thin films with controllable carrier densities were obtained by ozone molecular beam epitaxy (MBE). We fabricated Ga<sub>2</sub>O<sub>3</sub> metal-semiconductor field-effect transistors (MESFETs) and Schottky barrier diodes

(SBDs) from single-crystal Ga<sub>2</sub>O<sub>3</sub> substrates and MBE-grown epitaxial wafers. The MESFETs delivered excellent device performance including an off-state breakdown voltage ( $V_{br}$ ) of over 250 V, a low leakage current of only few  $\mu\text{A mm}^{-1}$ , and a high drain current on/off ratio of about four orders of magnitude. The SBDs also showed good characteristics such as near-unity ideality factors and high reverse  $V_{br}$ . These results indicate that Ga<sub>2</sub>O<sub>3</sub> can potentially meet or even exceed the performance of Si and typical widegap semiconductors such as SiC or GaN for ultrahigh-voltage power switching applications.

© 2013 WILEY-VCH Verlag GmbH & Co. KGaA, Weinheim

**1 Introduction** The worldwide quests for stable energy supplies and reduced greenhouse gas emissions in the near future have fueled demands for new energy sources to replace fossil fuels as well as ideas for revolutionary technologies to realize efficient energy generation and utilization. Power devices based on wide-bandgap semiconductors such as SiC and GaN are capable of delivering higher breakdown voltage ( $V_{br}$ ) and lower loss than Si devices, and have been intensively studied as alternative technologies for efficient power switching. However, both SiC and GaN power devices are unamenable to mass production since high-quality substrates are expensive, leaving ample room for new materials to enter the market. A new oxide semiconductor – gallium oxide (Ga<sub>2</sub>O<sub>3</sub>) – turns out to be an ideal material for power devices in ultrahigh-voltage switching applications. The superior material properties of Ga<sub>2</sub>O<sub>3</sub>, including a bandgap much larger than those of SiC and GaN, promise power devices with even higher  $V_{br}$  and efficiency than their SiC and GaN counterparts. The other important feature of Ga<sub>2</sub>O<sub>3</sub> is that native substrates can be fabricated from bulk single crystals synthesized by the same melt-growth methods employed for

manufacturing sapphire substrates. As large and high-quality sapphire substrates are now being manufactured in a low-cost commercial process in numbers rivaling those for Si, it can be expected that melt-grown Ga<sub>2</sub>O<sub>3</sub> substrates will reap the same benefits. Nevertheless, research and development (R&D) on Ga<sub>2</sub>O<sub>3</sub> devices has lagged since most researchers have failed to exploit the material's excellent properties. With the vision that Ga<sub>2</sub>O<sub>3</sub> power devices can potentially surpass SiC and GaN in not only device performance but also cost effectiveness, we began pioneering work on Ga<sub>2</sub>O<sub>3</sub> power devices in 2010. We have already developed various elemental technologies and achieved several important milestones, most notably the world's first demonstration of single-crystal Ga<sub>2</sub>O<sub>3</sub> transistors [1]. In this paper, we introduce the current status of our activities on Ga<sub>2</sub>O<sub>3</sub> power devices and the future prospects of this new technology.

**2 Crystal structure and material properties of β-Ga<sub>2</sub>O<sub>3</sub>** Ga<sub>2</sub>O<sub>3</sub> crystals exhibit polytypism with five confirmed polytypes (α, β, γ, δ, ε). The β-polytype shown in Fig. 1 is believed to be the most stable, while the other polytypes are metastable. β-Ga<sub>2</sub>O<sub>3</sub> crystallizes into the

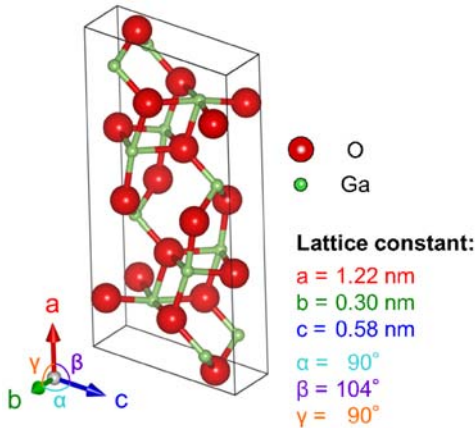


**Figure 1** Atomic unit cell of  $\beta$ -Ga<sub>2</sub>O<sub>3</sub>.

$\beta$ -gallia structure belonging to the monoclinic system. The bandgap of  $\beta$ -Ga<sub>2</sub>O<sub>3</sub> is 4.7–4.9 eV [2–4]. Semi-insulating Ga<sub>2</sub>O<sub>3</sub> can be controllably doped with Sn or Si to obtain electron densities ( $n$ ) from  $10^{16}$  to  $10^{19}$  cm<sup>-3</sup> [5–8]. In contrast, there has been no clear evidence of hole conduction in Ga<sub>2</sub>O<sub>3</sub>. The extrapolated experimental bulk electron mobility of Ga<sub>2</sub>O<sub>3</sub> reaches a relatively high value of about 300 cm<sup>2</sup> V<sup>-1</sup> s<sup>-1</sup> for  $n = 10^{15}$ – $10^{16}$  cm<sup>-3</sup>, which is typical for the drift layers of vertical power transistors and diodes [9]. This relatively high mobility is in agreement with theoretical calculations showing that the electron effective mass of Ga<sub>2</sub>O<sub>3</sub> is 0.23–0.34 $m_0$  ( $m_0$ : free electron mass), which is comparable to those of conventional widegap (3–4 eV) semiconductors [4, 7, 10].

**3 Performance prospect of Ga<sub>2</sub>O<sub>3</sub> power devices** With a bandgap wider than those of SiC and GaN,  $\beta$ -Ga<sub>2</sub>O<sub>3</sub> promises power transistors and diodes with excellent characteristics including high  $V_{br}$ , high power capacity, and low loss (*i.e.*, high efficiency). Table 1 compares the important material properties of  $\beta$ -Ga<sub>2</sub>O<sub>3</sub> with those of major semiconductors. The estimated breakdown electric field of Ga<sub>2</sub>O<sub>3</sub> is 8 MV cm<sup>-1</sup>, which is three times larger than that of either SiC or GaN. This high breakdown field is the most attractive attribute of Ga<sub>2</sub>O<sub>3</sub> for power devices, because Baliga’s figure of merit (FOM) – the basic parameter to show how suitable a material is for power devices – is proportional to the cube of the breakdown field,

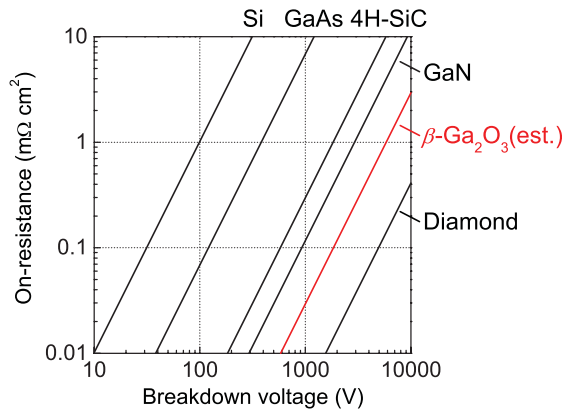


**Figure 2** Benchmarking the theoretical ideal performance limits of  $\beta$ -Ga<sub>2</sub>O<sub>3</sub> power devices against other major semiconductors.

but only linearly proportional to mobility. The theoretical limits of on-resistances as a function of  $V_{br}$  for Ga<sub>2</sub>O<sub>3</sub> and representative semiconductors as plotted in Fig. 2 suggest that the on-resistance of Ga<sub>2</sub>O<sub>3</sub> devices can be one order of magnitude lower than those of SiC and GaN devices at the same  $V_{br}$ . The thermal conductivity of Ga<sub>2</sub>O<sub>3</sub> strongly depends on the crystal orientation due to its asymmetric crystal structure. In our experiments, the [010] direction has the highest value of 0.23 W cm<sup>-1</sup> K<sup>-1</sup>, which is about twice as large as that in the [100] direction [11]. However, it is still much smaller than those of the other semiconductors and thus a clear weak point of Ga<sub>2</sub>O<sub>3</sub> in terms of power device applications.

**4 Production of single-crystal Ga<sub>2</sub>O<sub>3</sub> substrates** The superiority of Ga<sub>2</sub>O<sub>3</sub> devices for mass production stems from the availability of affordable native substrates fabricated from melt-grown bulk crystals at low cost and with low energy consumption [12–14]. A melt-growth technology known as edge-defined film-fed growth (EFG) has a good track record of producing large sapphire wafers of over 6 inch in diameter. This method will be especially useful for high-volume production of Ga<sub>2</sub>O<sub>3</sub> substrates using the same system configuration as for sapphire growth since it does not require a high-temperature or high-pressure environment, conserves source materials, and is easily scalable to large wafer diameters. In contrast, SiC and GaN bulk crystals and substrates are produced by energy-intensive and cost-

**Table 1** Material properties of major semiconductors and  $\beta$ -Ga<sub>2</sub>O<sub>3</sub>.

	Si	GaAs	4H-SiC	GaN	diamond	$\beta$ -Ga <sub>2</sub> O <sub>3</sub>
bandgap $E_g$ (eV)	1.1	1.4	3.3	3.4	5.5	4.7–4.9
electron mobility $\mu$ (cm <sup>2</sup> V <sup>-1</sup> s <sup>-1</sup> )	1400	8000	1000	1200	2000	300
breakdown field $E_b$ (MV cm <sup>-1</sup> )	0.3	0.4	2.5	3.3	10	8
relative dielectric constant $\epsilon$	11.8	12.9	9.7	9.0	5.5	10
Baliga’s FOM $\epsilon\mu E_b^3$	1	15	340	870	24 664	3444
thermal conductivity (W cm <sup>-1</sup> K <sup>-1</sup> )	1.5	0.55	2.7	2.1	10	0.23 [010] 0.13 [100]

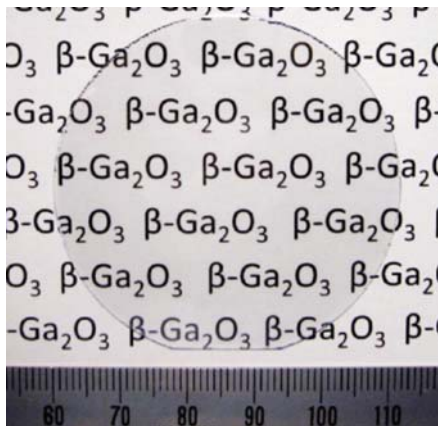


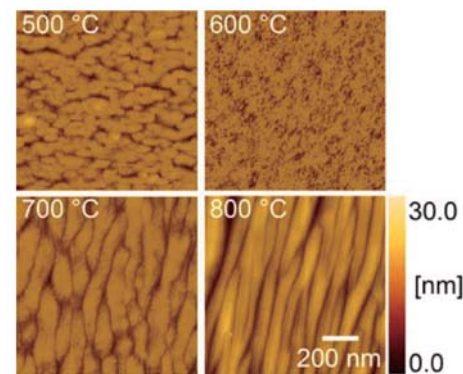
**Figure 3** Photograph of 2-inch-diameter single-crystal  $\text{Ga}_2\text{O}_3$  wafer.

prohibitive methods such as sublimation, vapor phase epitaxy, and high-pressure synthesis [15–17]. Figure 3 shows a 2-inch-diameter single-crystal  $\text{Ga}_2\text{O}_3$  wafer produced in our laboratory. The crystal quality of the  $\text{Ga}_2\text{O}_3$  wafer is very good, with a full-width at half-maximum of the X-ray diffraction rocking curve as narrow as 19 arcsec and a dislocation density on the order of  $10^4 \text{ cm}^{-2}$  as characterized by surface etch pits. The surface of the wafer was atomically flat after chemical-mechanical polishing with a small root-mean-square (RMS) surface roughness of 0.11 nm. Undoped  $\text{Ga}_2\text{O}_3$  substrates show n-type conductivity due to unintentional Si incorporation from the  $\text{Ga}_2\text{O}_3$  powder source (5 N). Compensation doping with deep acceptors such as Mg renders these materials semi-insulating.

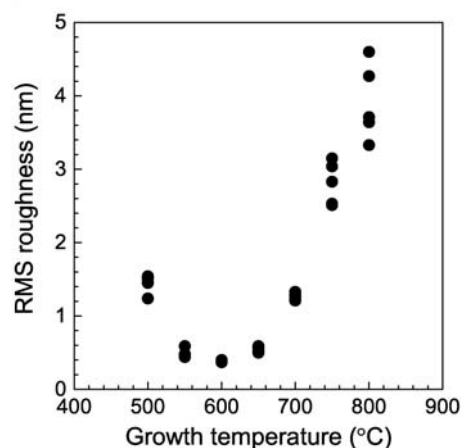
### 5 Epitaxial growth of $\text{Ga}_2\text{O}_3$ thin films by ozone

**MBE** We have developed homoepitaxy of Sn-doped n-type  $\beta\text{-Ga}_2\text{O}_3$  on native substrates by molecular-beam epitaxy (MBE) [9, 18]. The substrates used were unintentionally n-doped  $\beta\text{-Ga}_2\text{O}_3$  (010) fabricated from a bulk synthesized by the floating-zone (FZ) method. Ga and Sn (n-type dopant) were, respectively, supplied from 7 N Ga metal and 4 N  $\text{SnO}_2$  powder heated in conventional Knudsen cells (K-cells). The oxygen source was an ozone(5%)–oxygen (95%) gas mixture. Growth temperatures ranging from 500 to 800 °C were attempted to investigate their effects on surface morphology and doping. The growth rate and film thickness were  $600 \text{ nm h}^{-1}$  and 600 nm, respectively.

The surface morphologies of the epitaxial films were evaluated by atomic force microscopy (AFM). Figure 4(a) shows the AFM images of  $\text{Ga}_2\text{O}_3$  epitaxial films grown at various temperatures. Step bunching along the [100] direction is observed for growth temperatures higher than 700 °C, and the effect becomes more pronounced with increasing growth temperatures. On the other hand, a low growth temperature of 500 °C results in a rough surface due to three-dimensional growth. The RMS surface roughness values of the  $\text{Ga}_2\text{O}_3$  epitaxial films estimated from  $1 \times 1 \mu\text{m}^2$  AFM scans are plotted as a function of growth



(a)



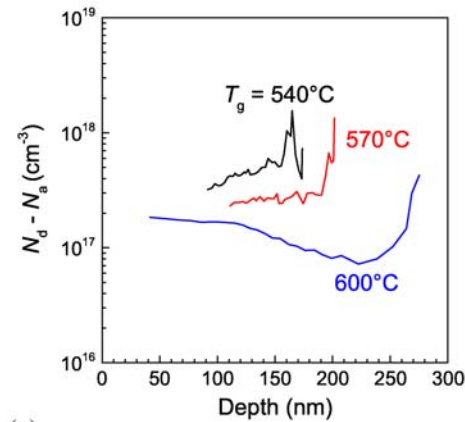
(b)

**Figure 4** (a) Surface morphologies of MBE  $\text{Ga}_2\text{O}_3$  thin films grown at various temperatures as observed by AFM and (b) RMS surface roughness of the  $\text{Ga}_2\text{O}_3$  film as a function of growth temperature.

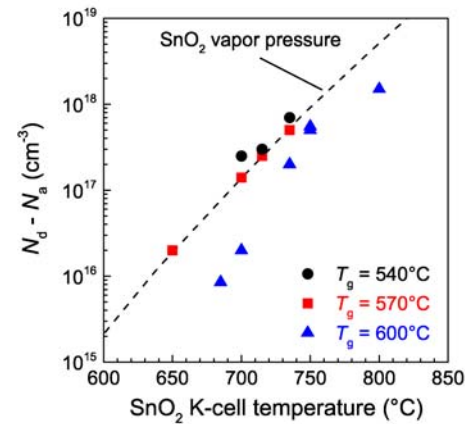
temperature in Fig. 4(b). The smoothest films were grown at 550–650 °C.

Electrochemical capacitance–voltage ( $C$ – $V$ ) measurements were employed to evaluate the dependence of effective donor concentration ( $N_d - N_a$ ) on growth parameters. Figure 5 (a) shows the  $N_d - N_a$  depth profiles in three Sn-doped  $\text{Ga}_2\text{O}_3$  epitaxial films grown at 540, 570, and 600 °C, respectively. The  $N_d - N_a$  in Sn-doped  $\text{Ga}_2\text{O}_3$  as a function of  $\text{SnO}_2$  K-cell temperature is shown in Fig. 5(b). Uniform doping concentrations along the growth direction that corresponded to the  $\text{SnO}_2$  vapor pressure were achieved for the samples grown at 540 and 570 °C. In contrast, a delay in doping at the initial stage of the 600 °C growth due likely to Sn segregation was revealed in Fig. 5(a), causing the lower-than-expected average  $N_d - N_a$  in the sample according to Fig. 5(b). These results indicate that a growth temperature below 570 °C is necessary for accurate control of carrier density.

We have optimized the structural and electrical properties of MBE-grown Sn-doped  $\beta\text{-Ga}_2\text{O}_3$  homoepitaxial films. High-quality epilayers with both smooth surfaces and uniform doping profiles were obtained at growth temperatures of 540–570 °C.



(a)

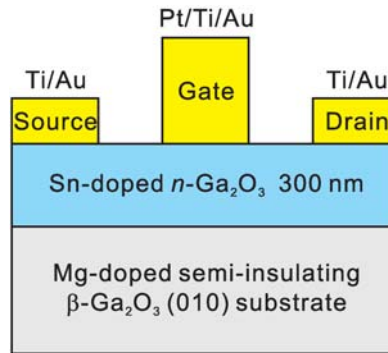


(b)

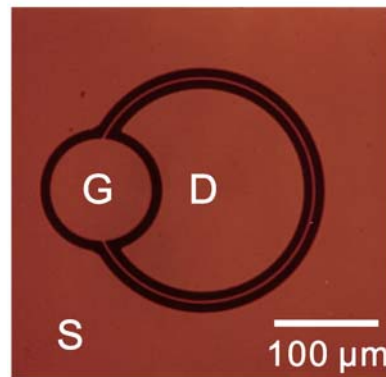
**Figure 5** (a) Depth profiles of  $N_d - N_a$  in Sn-doped  $\text{Ga}_2\text{O}_3$  epitaxial films grown at various temperatures estimated by electrochemical  $C-V$  measurements and (b)  $N_d - N_a$  of Sn-doped  $\text{Ga}_2\text{O}_3$  films as a function of  $\text{SnO}_2$  K-cell temperature.

**6  $\text{Ga}_2\text{O}_3$  MESFETs** Transistor action for single-crystal  $\text{Ga}_2\text{O}_3$  devices was demonstrated using simple metal-semiconductor field-effect transistor (MESFET) structures [1]. Sn-doped  $n\text{-Ga}_2\text{O}_3$  MESFET channel layers were grown on Mg-doped semi-insulating  $\beta\text{-Ga}_2\text{O}_3$  (010) FZ substrates by ozone MBE. Figure 6(a) shows a cross-sectional schematic illustration of the  $n\text{-Ga}_2\text{O}_3$  MESFET. To form Ohmic contacts, reactive ion etching (RIE) using a gas mixture of  $\text{BCl}_3$  and Ar was first performed to reduce the contact resistance substantially, followed by evaporation of Ti/Au. Then, Schottky gates were fabricated by Pt/Ti/Au deposition and lift off. The surface was left unpassivated. The gate length, source-drain spacing, and diameter of the inner circular drain electrode were 4, 20, and 200  $\mu\text{m}$ , respectively. We employed a circular FET pattern as shown in the optical micrograph of a fabricated device in Fig. 6(b), since a device isolation technique has not yet been developed.

Figure 7(a) and (b) show the DC output current–voltage ( $I-V$ ) and transfer characteristics, respectively, of the  $\text{Ga}_2\text{O}_3$



(a)



(b)

**Figure 6** (a) Cross-sectional schematic illustration and (b) optical micrograph of  $\text{Ga}_2\text{O}_3$  MESFET.

MESFET. The drain current ( $I_d$ ) was effectively modulated by a gate voltage ( $V_g$ ) with a sharp pinch-off characteristic. The device exhibited a maximum  $I_d$  of 16 mA at a drain voltage ( $V_d$ ) of 40 V and a  $V_g$  of +2 V. The three-terminal destructive breakdown in the off-state, which resulted in burned gate electrodes, occurred at a  $V_d$  of over 250 V. Transconductance peaked at 1.4 mS for  $V_d = 40$  V. The off-state drain leakage current ( $I_{\text{off}}$ ) was as small as 3  $\mu\text{A}$ , resulting in a high  $I_d$  on/off ratio of about  $10^4$ . The  $I_{\text{off}}$  was comparable to the gate leakage current, indicating that leakage through the semi-insulating  $\text{Ga}_2\text{O}_3$  substrate was negligible. Furthermore, most gate leakage current could be attributed to the large 100- $\mu\text{m}$ -diameter gate pad [Fig. 6(b)], and the actual leakage through the gate finger should be lower by at least one order of magnitude. Therefore, the  $I_{\text{off}}$  can be effectively suppressed simply by optimizing the device configuration. While our first  $\text{Ga}_2\text{O}_3$  MESFETs are inferior to the state-of-the-art SiC and GaN devices, their performance was comparable to or better than that of GaN MESFETs in the early 1990s [19, 20]. The high  $V_{\text{br}}$  and low leakage current of these transistors indicate their great potential as power devices.

**7  $\text{Ga}_2\text{O}_3$  SBDs** Another important component for power electronics is the Schottky barrier diode

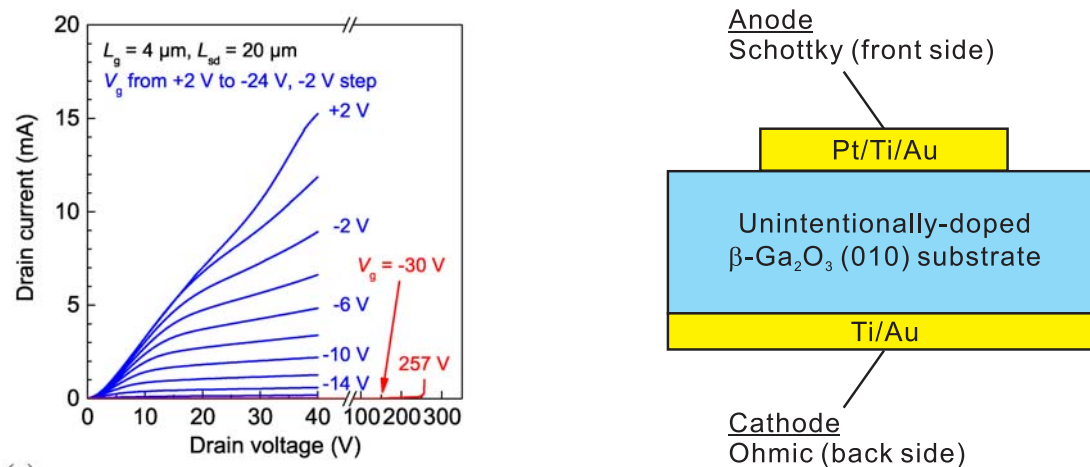


**Figure 8** Cross-sectional schematic illustration of Ga<sub>2</sub>O<sub>3</sub> SBD.

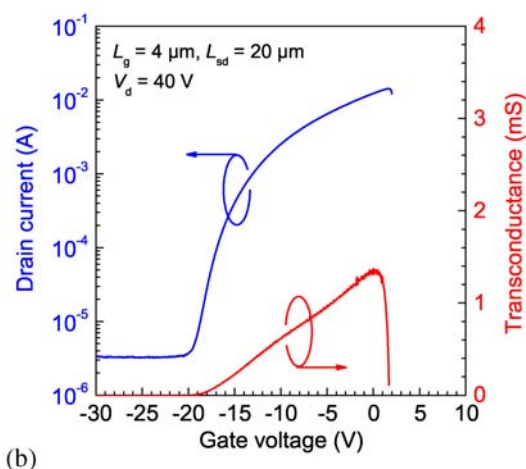


**Figure 7** (a) DC output  $I$ - $V$  curves and (b) transfer characteristics of Ga<sub>2</sub>O<sub>3</sub> MESFET.

(SBD) [21]. We fabricated simple SBDs on unintentionally n-doped single-crystal  $\beta$ -Ga<sub>2</sub>O<sub>3</sub> FZ substrates with a thickness of 600  $\mu\text{m}$ . The  $n$  was uniform along the thickness of the substrate but showed in-plane variation from  $3 \times 10^{16}$  to  $1 \times 10^{17} \text{ cm}^{-3}$  as evaluated by  $C$ - $V$  measurements. Figure 8 shows a cross-sectional schematic illustration of the Ga<sub>2</sub>O<sub>3</sub> SBD structure. Circular Schottky contacts with a diameter of 100  $\mu\text{m}$  were fabricated on the front side of the substrate as anode electrodes by standard photolithographic patterning, Pt/Ti/Au evaporation, and lift off. The cathode electrode (Ti/Au) was evaporated onto the backside of the substrate following an RIE treatment using a mixture of BCl<sub>3</sub> and Ar gases to decrease the Ohmic contact resistance.

Figure 9(a) and (b) plot the forward current density–voltage ( $J$ - $V$ ) characteristics of two different Ga<sub>2</sub>O<sub>3</sub> SBDs fabricated at different locations on the same substrate with  $n = 3 \times 10^{16}$  and  $5 \times 10^{16} \text{ cm}^{-3}$ , respectively. Note that the  $J$  value simply corresponds to the current divided by the anode

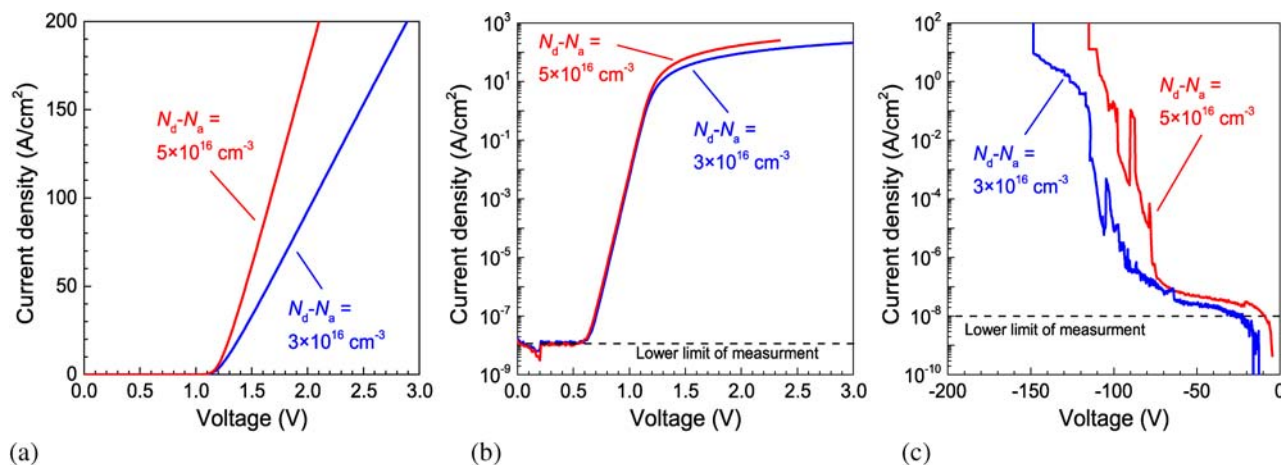


**Figure 9** (a, b) Forward (linear and semilog plot, respectively) and (c) reverse  $J$ - $V$  characteristics of Ga<sub>2</sub>O<sub>3</sub> SBDs.

electrode area. The near-unity ideality factors of 1.04–1.06 indicated the high crystal quality of the Ga<sub>2</sub>O<sub>3</sub> substrate and good Schottky interface property. A Schottky barrier height of 1.3–1.5 eV was extracted for the Pt/β-Ga<sub>2</sub>O<sub>3</sub> interface. Due to the low unintentional *n* and hence low substrate conductivity, the on-resistances (*R*<sub>on</sub>) of the Ga<sub>2</sub>O<sub>3</sub> SBDs, which was determined from the slope of the linear regions in Fig. 9(a), were relatively high at 7.85 and 4.30 mΩ cm<sup>2</sup> when compared with those of state-of-the-art SBDs based on other semiconductors. However, they can be readily improved by incorporating an n<sup>+</sup>-Ga<sub>2</sub>O<sub>3</sub> contact layer. Figure 9(c) shows the reverse *J–V* characteristics of the Ga<sub>2</sub>O<sub>3</sub> SBDs. The reverse *V*<sub>br</sub> values were about 150 and 115 V for *n* = 3 × 10<sup>16</sup> and 5 × 10<sup>16</sup> cm<sup>-3</sup>, respectively, which were reasonably high for these carrier densities considering the lack of surface passivation or edge termination.

**8 Conclusions** We propose a new oxide compound semiconductor Ga<sub>2</sub>O<sub>3</sub> as a promising candidate for power device applications because of its excellent material properties and suitability for mass production. Homoepitaxy of *n*-type Ga<sub>2</sub>O<sub>3</sub> thin films on β-Ga<sub>2</sub>O<sub>3</sub> (010) substrates by MBE with precise control of carrier density over the range of 10<sup>16</sup>–10<sup>19</sup> cm<sup>-3</sup> was demonstrated. Ga<sub>2</sub>O<sub>3</sub> MESFETs and SBDs were fabricated on single-crystal β-Ga<sub>2</sub>O<sub>3</sub> substrates. The MESFETs showed excellent device performance such as a three-terminal off-state *V*<sub>br</sub> of 250 V and an *I*<sub>d</sub> on/off ratio of about four orders of magnitude. The SBDs also exhibited good characteristics such as near-unity ideality factors and high reverse *V*<sub>br</sub>. These results indicate that Ga<sub>2</sub>O<sub>3</sub> can potentially meet or even exceed the performance of Si and typical widegap semiconductors such as SiC or GaN for ultrahigh-voltage power switching applications.

The R&D on Ga<sub>2</sub>O<sub>3</sub> power devices is at its early stage. Large-area Ga<sub>2</sub>O<sub>3</sub> wafers of over 4 inch in diameter are yet to be produced. Practical power switching equipment is best designed using more advanced transistors architectures such as normally-off vertical devices, which calls for further developments in epitaxial growth, doping, and device processing technologies. Our pioneering development of Ga<sub>2</sub>O<sub>3</sub> transistors and diodes paves the way for new high-performance devices that will advance the power semiconductor industry and reduce global energy consumption.

**Acknowledgement** This work was partially supported by “The research and development project for innovation technique of energy conservation” of the New Energy and Industrial Technology Development Organization (NEDO). It also made use of a research

grant from the PRESTO program of the Japan Science and Technology Agency (JST).

## References

- [1] M. Higashiwaki, K. Sasaki, A. Kuramata, T. Masui, and S. Yamakoshi, *Appl. Phys. Lett.* **100**, 013504 (2012).
- [2] H. H. Tippins, *Phys. Rev.* **140**, A316 (1965).
- [3] M. Orita, H. Ohta, M. Hirano, and H. Hosono, *Appl. Phys. Lett.* **77**, 4166 (2000).
- [4] H. He, R. Orlando, M. A. Blanco, R. Pandey, E. Amzallag, I. Baraille, and M. Rérat, *Phys. Rev. B* **74**, 195123 (2006).
- [5] N. Ueda, H. Hosono, R. Waseda, and H. Kawazoe, *Appl. Phys. Lett.* **70**, 3561 (1997).
- [6] E. G. Villora, K. Shimamura, Y. Yoshikawa, T. Ujiie, and K. Aoki, *Appl. Phys. Lett.* **92**, 202120 (2008).
- [7] J. B. Varley, J. R. Weber, A. Janotti, and C. G. Van de Walle, *Appl. Phys. Lett.* **97**, 142106 (2010).
- [8] K. Irmscher, Z. Galazka, M. Pietsch, R. Uecker, and R. Fornari, *J. Appl. Phys.* **110**, 063720 (2011).
- [9] K. Sasaki, A. Kuramata, T. Masui, E. G. Villora, K. Shimamura, and S. Yamakoshi, *Appl. Phys. Express* **5**, 035502 (2012).
- [10] K. Yamaguchi, *Solid State Commun.* **131**, 739 (2004).
- [11] E. G. Villora, K. Shimamura, T. Ujiie, and K. Aoki, *Appl. Phys. Lett.* **92**, 202118 (2008).
- [12] E. G. Villora, K. Shimamura, Y. Yoshikawa, K. Aoki, and N. Ichinose, *J. Cryst. Growth* **270**, 420 (2004).
- [13] H. Aida, K. Nishiguchi, H. Takeda, N. Aota, K. Sunakawa, and Y. Yaguchi, *Jpn. J. Appl. Phys.* **47**, 8506 (2008).
- [14] Z. Galazka, R. Uecker, K. Irmscher, M. Albrecht, D. Klimm, M. Pietsch, M. Brützm, R. Bertram, S. Ganschow, and R. Fornari, *Cryst. Res. Technol.* **45**, 1229 (2010).
- [15] St. G. Müller, R. C. Glass, H. M. Hobgood, V. F. Tsvetkov, M. Brady, D. Henshall, J. R. Jenny, D. Malta, and C. H. Carter, Jr., *J. Cryst. Growth* **211**, 325 (2000).
- [16] K. Fujito, S. Kubo, H. Nagaoka, T. Mochizuki, H. Namita, and S. Nagao, *J. Cryst. Growth* **311**, 3011 (2009).
- [17] R. Dwiliński, R. Doradziński, J. Garczyński, L. P. Sierżputowski, A. Puchalski, Y. Kanbara, K. Yagi, H. Minakuchi, and H. Hayashi, *J. Cryst. Growth* **311**, 3015 (2009).
- [18] K. Sasaki, M. Higashiwaki, A. Kuramata, T. Masui, and S. Yamakoshi, *Abstr. of 40th Int. Symp. Compound Semiconductors, TuB3-2* (2013).
- [19] M. Asif Khan, J. N. Kuznia, A. R. Bhattarai, and D. T. Olson, *Appl. Phys. Lett.* **62**, 1786 (1993).
- [20] S. C. Binari, L. B. Rowland, W. Kruppa, G. Kelner, K. Doverspike, and D. K. Gaskill, *Electron. Lett.* **30**, 1248 (1994).
- [21] K. Sasaki, M. Higashiwaki, A. Kuramata, T. Masui, and S. Yamakoshi, *IEEE Electron Device Lett.* **34**, 493 (2013).